A comparative study of spinel structured Mn_3O_4, Co_3O_4 and Fe_3O_4 nanoparticles in catalytic oxidation of phenolic contaminants in aqueous solutions

*Edy Saputra[1,2], Syaifullah Muhammad[1,3], Hongqi Sun[1], Ha-Ming Ang[1], Moses O. Tadé[1], Shaobin Wang[1,]**

[1]*Department of Chemical Engineering and CRC for Contamination Assessment and Remediation of the Environment (CRC-CARE), Curtin University, GPO Box U1987, Perth, WA 6845, Australia*

[2]*Department of Chemical Engineering, Riau University, Pekanbaru 28293, Indonesia*

[3]*Department of Chemical Engineering, Syiah Kuala University, Banda Aceh, Indonesia*

Abstract

Spinel structured Mn_3O_4, Co_3O_4 and Fe_3O_4 nanoparticles were prepared, characterised, and tested in degradation of aqueous phenol in the presence of peroxymonosulfate. It was found that Mn_3O_4 and Co_3O_4 nanoparticles are highly effective in heterogeneous activation of peroxymonosulfate to produce sulphate radicals for phenol degradation. The activity shows an order of Mn_3O_4 > Co_3O_4 > Fe_3O_4. Mn_3O_4 could fast and completely remove phenol in about 20 min, at the conditions of 25 ppm phenol, 0.4 g/L catalyst, 2 g/L oxone®, and 25 ^oC. A pseudo first order model would fit to phenol degradation kinetics and activation energies on Mn_3O_4 and Co_3O_4 were obtained as 38.5 and 66.2 kJ/mol, respectively. In addition, Mn_3O_4 exhibited excellent catalytic stability in several runs, demonstrating that Mn_3O_4 is a promising catalyst alternative to toxic Co_3O_4 for water treatment.

Key words: Metal oxides, Phenol degradation, Spinel structure, Mn_3O_4, Co_3O_4, and Fe_3O_4

---

*Correspondence author. Email: Shaobin.wang@curtin.edu.au

1. Introduction

Phenol and its derivatives are important water pollutants due to their strong toxicity to many living organisms even at low concentrations [1]. These chemicals can be discharged from many industries as by-products such as petroleum refining, petrochemical, pharmaceutical, plastic and pesticide industries [2, 3]. In many countries, the maximum threshold allowed for phenol in water streams is less than 1 mg/L, for instance 0.5 mg/L for Australia wastewaters [4, 5]. Therefore, the phenol containing wastewaters have to be treated before discharged into the environment.

Currently, conventional wastewater treatment technology has been proven to be limited in treating toxic organic compounds because degradation of various pollutants is often very slow or ineffective and not environmentally compatible [6, 7]. One promising technology that can be used as an effective process to completely degrade organic compounds in aqueous media is advanced oxidation processes (AOPs). AOPs are based on the generation of reactive species, such as hydroxyl radicals, that have a strong oxidizing potential for mineralizing organic pollutants into simple compounds, CO_2 and H_2O [8, 9]. Apart from hydroxyl radicals, sulphate radicals have also been recently suggested as an alternative due to their higher oxidation potential.

Homogeneous catalysts are commonly more efficient compared to solid or heterogeneous catalysts because every single catalytic entity can act as a single active site. This characteristic makes homogeneous catalysts intrinsically more active and selective [10]. However, recovery of the catalysts needs further processes for separation of the homogeneous catalysts. Moreover, most of the dissolved metal catalysts are harmful to the environment. This disadvantage can be overcome by using heterogeneous catalysts, in which the catalysts will be recoverable and reusable [11].

In most previous investigations, homogeneous Co^{2+}/peroxymonosulfate (PMS, HSO_5^-) has been found to be an effective route of AOP for sulphate radical production and oxidation of various organics [12-17]. However, a major issue in using Co^{2+} metal ions is the toxicity and health problems to humans such as asthma and pneumonia [18]. Therefore, metal oxide catalysts for

activation of PMS, such as Co_3O_4 [19, 20], Co exchanged zeolites [21], supported Co_3O_4 [22-31], and $CoFe_2O_4$ [30, 32] have been proposed to overcome this drawback. Recently, RuO_2 [33] and MnO_2 [34] have also been reported to be effective for phenol degradation.

Co_3O_4, Fe_3O_4, and Mn_3O_4 are important oxides with spinel structure consisting of M^{2+} and M^{3+} ions. They are active in generating hydroxyl radicals via Fenton-like reaction for advanced oxidation processes. However, unlike Co_3O_4, Fe_3O_4 and Mn_3O_4 are less toxic and more environmental-benign catalysts in water treatment. Although Co_3O_4 and Fe_3O_4 have been tested in activation of PMS, no investigation has been reported on Mn_3O_4 for PMS activation. In this research, three metal oxides, Mn_3O_4, Co_3O_4 and Fe_3O_4, were synthesized in two ways, hydrothermal and solvothermal methods. Their physicochemical and morphological properties were characterized. The prepared metal oxide materials were then employed as catalysts for heterogeneous generation of sulphate radicals for phenol mineralization in solution. It was found that Mn_3O_4 presented superior performance to Co_3O_4 and Fe_3O_4. In addition, several key parameters in the evaluation of kinetic study such as phenol concentration, catalyst loading, PMS concentration and temperature were investigated.

2. Experimental methods

2.1. Material synthesis.

A nano-sized Mn_3O_4 sample was prepared by a solvothermal method reported by Zhang et al. [35]. In this synthesis, 1.0 g potassium permanganate was dissolved in 60 mL aqueous ethanol (60%) at room temperature to form a homogeneous solution. The solution was transferred into a 125 mL Teflon-lined stainless steel autoclave, sealed and maintained at 120 ^oC for 8 h. The resulting precipitates were filtered and washed with distilled water and dried in air at 80 ^oC overnight. The second sample, nanostructured Co_3O_4, was prepared by a hydrothermal method [36]. Typically, $Co(NO_3)_2$•$6H_2O$ (5 mmol) and $CO(NH_2)_2$ (25 mmol) were dissolved in 50 mL of distillate water under stirring. The solution was transferred into a 125 mL Teflon-lined stainless steel autoclave,

sealed and maintained at 120 ^{o}C for 5 h. The resulted precipitates were filtered and washed with water and dried in air at 80 ^{o}C overnight. Then, the dried solid was calcined at 400 ^{o}C under air for 4 h. Fe_3O_4 nanoparticles were obtained by a solvothermal method [37]. Typically, ferric sulfate (0.45 g), sodium acetate anhydrous (1.2 g), and poly(vinylpyrrolidone) (average Mw = 40 000, 0.3 g) were dissolved in ethylene glycol (25 mL) under stirring. The mixture was then transferred into a 45 mL Teflon-lined stainless steel autoclave, sealed and maintained at 200 ^{o}C for 8 h. The resulting precipitates were filtered and washed with water and dried in air at 80 ^{o}C for 24 h.

2.2. Characterization of catalysts.

Catalysts were characterized by X-ray diffraction (XRD), N_2 adsorption/desorption isotherms, and scanning electron microscopy (SEM). XRD patterns were obtained on a Bruker D8 (Bruker-AXS, Karlsruhe, Germany) diffractometer using filtered Cu Kα radiation source (λ = 1.54178 Å), with accelerating voltage 40 kV, current 30 mA and scanned at 2θ from 5 to 100^{o}. N_2 adsorption/desorption was measured using a Micromeritics Tristar 3000 to obtain pore volume and Brunauer-Emmett-Teller (BET) specific surface area. Prior to measurement the samples were degassed at 120 ^{o}C for 5 h under vacuum condition. The external morphology and chemical compositions of the samples were observed on a ZEISS NEON 40EsB scanning electron microscope (SEM) equipped with an energy dispersive spectrometer (SEM-EDS).

2.3. Catalytic activity tests.

Phenol degradation tests were carried out in a 1-L glass beaker with 500 mL containing 25, 50, 75 and 100 mg/L of phenolic solutions. The reaction mixture was stirred constantly at 400 rpm. Firstly, a fixed amount of peroxymonosulfate (oxone®, DuPont's triple salt: $2KHSO_5 \bullet KHSO_4 \bullet K_2SO_4$, Sigma-Aldrich) was added into the solution for a while, then a catalyst was added into the solution to start the oxidation reaction of phenol. At certain time, 0.5 mL of water sample was withdrawn from the mixture using a syringe filter of 0.45 μm and then mixed with 0.5 mL of pure methanol to quench the reaction. The concentration of phenol was analyzed using a Varian HPLC with a UV

detector at λ = 270 nm. The column used was C-18 with mobile phase of 30% CH_3CN and 70% ultrapure water. For selected samples, total organic carbon (TOC) was obtained using a Shimadzu TOC-5000 CE analyzer.

3. Results and discussion

3.1. Characterization of oxide catalysts.

Fig. S1 shows XRD patterns of Mn_3O_4, Co_3O_4 and Fe_3O_4 catalysts. The three samples present different crystalline peaks. The peaks in Fig. S1a match well with those from the JCPDS card (19-0629) for magnetite Fe_3O_4. The diffraction peaks in Fig. S1b are the same as those from the JCPDS card (24-0734) for Mn_3O_4. Meanwhile, the diffractions in Fig. S1c are similar to those from the JCPDS card (43-1003) for Co_3O_4.

Fig. 1 shows N_2 adsorption/desorption isotherms of three oxide catalysts and their textural properties are presented in Table 1. Mn_3O_4 presents the highest surface area (184.6 $m^2.g^{-1}$) and pore volume (0.772 $cm^3.g^{-1}$). Co_3O_4 and Fe_3O_4 show the similar surface area. In addition, Mn_3O_4 has the smallest average pore radius at 8 Å while other two catalysts (Co_3O_4 and Fe_3O_4) have a larger average pore size around 200 Å, suggesting most of their pores are macro size.

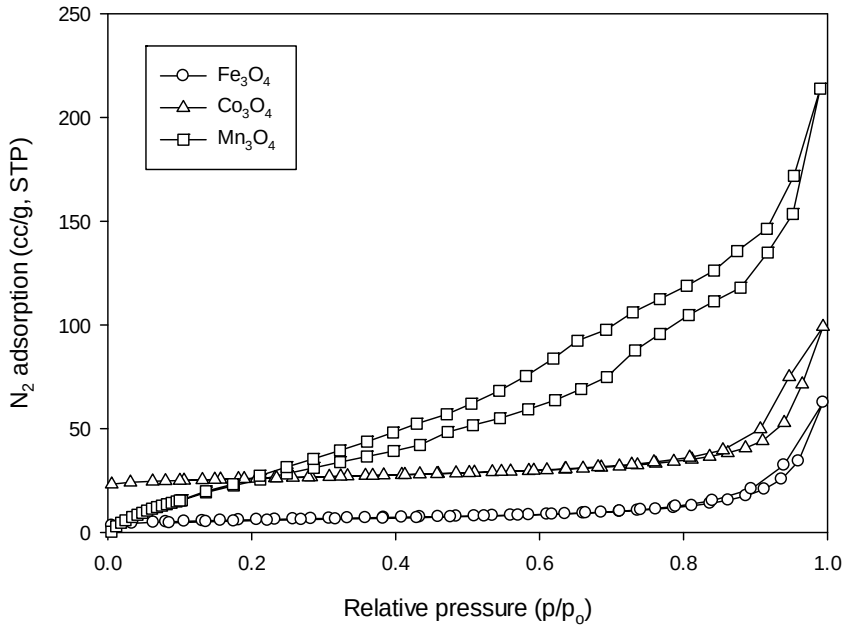

Fig. 1 N_2 adsorption isotherms of Fe_3O_4, Mn_3O_4, and Co_3O_4.

Table 1. Surface area, pore volume and pore radius of oxide catalysts.

Catalyst	Surface area (S_{BET}, $m^2.g^{-1}$)	Pore volume ($cm^3.g^{-1}$)	Average pore radius (Å)
Fe_3O_4	21.4	0.096	180
Mn_3O_4	184.6	0.772	8
Co_3O_4	20.0	0.120	240

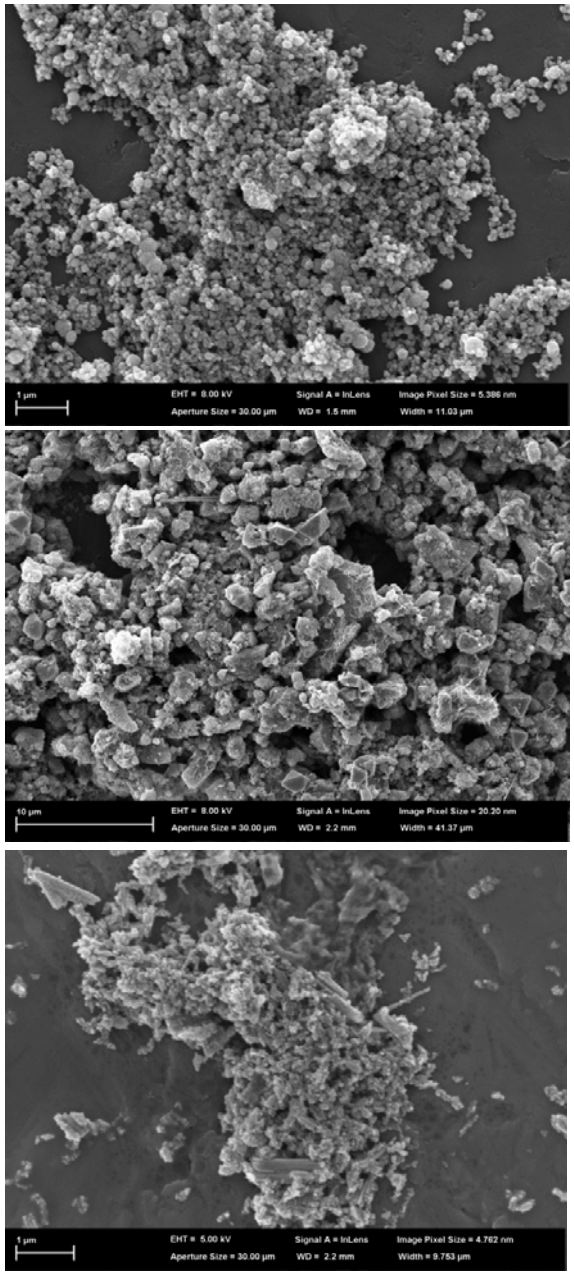

(a)

(b)

(c)

Fig. 2 SEM images of oxide catalysts. (a) Fe_3O_4, (b) Mn_3O_4, and (c) Co_3O_4.

Fig. 2 presents SEM images of three oxide catalyst samples. As seen, the morphology of Fe_3O_4 particles in the uniform size with spherical shape. The particle size is about 0.05-0.2 μm. Mn_3O_4 shows a larger particle size varying in a range of 0.15-2.5 μm. Another oxide (Co_3O_4) shows the particle size at about 0.02-0.25 μm.

3.2. Preliminary study of phenol oxidation using oxide catalysts.

The adsorption and degradation of phenol on Fe_3O_4, Mn_3O_4, and Co_3O_4 are presented in Fig. 3. In adsorption tests, all catalysts can adsorb phenol compound at low efficiency. Among the catalysts, Mn_3O_4 has the highest efficiency in phenol adsorption with 15% removal in 90 min prior to reaching equilibrium. Meanwhile, Co_3O_4 has a lower adsorption efficiency with 10% removal in 90 min. Mn_3O_4 has much higher surface area and pore volume than others, resulting in higher phenol adsorption. In the presence of oxone® without a catalyst, no phenol degradation occurred, indicating that oxone® itself could not produce sulfate radicals to induce phenol oxidation.

In catalytic oxidation tests, phenol degradation would only occur when catalyst and oxidant were simultaneously present in the solution. In a comparison of three catalyst performances, Co_3O_4 and Mn_3O_4 are effective in activating oxone® to generate sulfate radicals. Co_3O_4-oxone® system exhibited similar efficiency to Mn_3O_4-oxone®, presenting fast and complete phenol removal in 20 min. In contrary, Fe_3O_4-oxone® system presented much low degradation of phenol at less than 15% removal in 90 min. Thus, the order of catalytic activity of the catalysts is as follows, $Mn_3O_4 \sim Co_3O_4 > Fe_3O_4$. In addition, TOC removal in Co_3O_4-oxone® and Mn_3O_4-oxone® systems were also examined and about 68% and 50% of TOC reduction were obtained within 60 min, respectively.

The heterogeneous activation of PMS by Co_3O_4 has been previously investigated and the reactions were proposed in Eqs.(1-2)[19]. Due to the similar chemical structure of Fe_3O_4 and Mn_3O_4 to Co_3O_4, activation of PMS by Mn_3O_4 and Fe_3O_4 will follow the same routes. As shown in the reactions, redox reactions are involved in sulfate radical generation and the redox potential of M^{2+}/M^{3+} will be an important factor. The standard reduction potentials (E^0) of Co^{3+}/Co^{2+},

Mn^{3+}/Mn^{2+}, and Fe^{3+}/Fe^{2+} are 1.92, 1.54, and 0.77 V, respectively [38]. Due to higher value of E^0, Mn_3O_4 and Co_3O_4 exhibit high activity. In addition, Anipsitakis and Dionysiou [38] investigated homogeneous activation of PMS by several metal ions, Fe^{2+}, Fe^{3+}, Co^{2+}, Mn^{2+}, Ni^{2+}, Ru^{3+}, Ce^{3+}, and Ag^{+}, for 2,4-dichlorophenol degradation. They found that Co^{2+} and Ru^{3+} are the best metal catalysts for the activation of PMS. Co^{2+}, Ru^{3+}, and Fe^{2+} interact with PMS to produce freely diffusive sulfate radicals while Mn^{2+}, Ni^{2+}, and Ce^{3+} with PMS generate caged or bound to the metal sulfate radicals. For heterogeneous oxidation of phenol, activation of PMS occurred on the surface of oxide particles. BET measurement and adsorption tests showed Mn_3O_4 has higher surface area and phenol adsorption. The bounded sulfate radicals on Mn_3O_4 will be easily reacted with surface adsorbed phenol, resulting in more active in phenol degradation.

$$HSO_5^- + 2\ MO \rightarrow SO_4^{-\bullet} + H^+ + M_2O_3 \qquad M = Fe, Co, Mn \qquad (1)$$

$$HSO_5^- + M_2O_3 \rightarrow SO_5^{-\bullet} + OH^- + 2\ MO \qquad (2)$$

Anipsitakis and Dionysiou tested various commercial Co_3O_4 for heterogeneous activation of PMS for 2,4-dichlorophenol degradation and proposed that both CoO and Co_2O_3 contained in Co_3O_4 are responsible for PMS activation [19]. At the conditions of 20 mg/L 2,4-DCP, 0.19 g/L Co_3O_4, 72-99% conversion of 2,4-dichlorophenol could be achieved in 30 min. Some other investigations using unsupported Co oxide heterogeneous catalysts have been carried out in activation of PMS for oxidation of organic toxics in water. Liang et al. [39] studied a nanostructured Co_3O_4 which was synthesized by solution combustion for heterogeneous activation of oxone® to generate sulfate radicals ($SO_5^{-\bullet}$, and $SO_4^{-\bullet}$) for phenol degradation. They found that Co_3O_4 could only achieve 50% phenol removal at phenol concentration of 25 ppm within 240 min. Ding et al. [40] used nano-Co_3O_4 with oxone® for a dye (methylene blue, MB) degradation at 20 μmol/L. The nano-Co_3O_4 could achieve 40% MB removal in 30 min. Chen et al. [41] studied Mn_3O_4 nanoparticles with ozone for phenol degradation at 100 mg/L. It was reported that 80% phenol removal could be

achieved in 60 min. Previously, we tested a mesoporous MnO_2 for activation of oxone® to degrade phenol and 100% phenol decomposition occurred in 150 min under the similar conditions in this investigation [34]. Therefore, it is seen that synthesized Co_3O_4 and Mn_3O_4 with oxone® in this investigation presented much higher activity in phenol degradation. Due to their high activity, further investigations on Co_3O_4 and Mn_3O_4 were carried out to understand the effects of operating conditions.

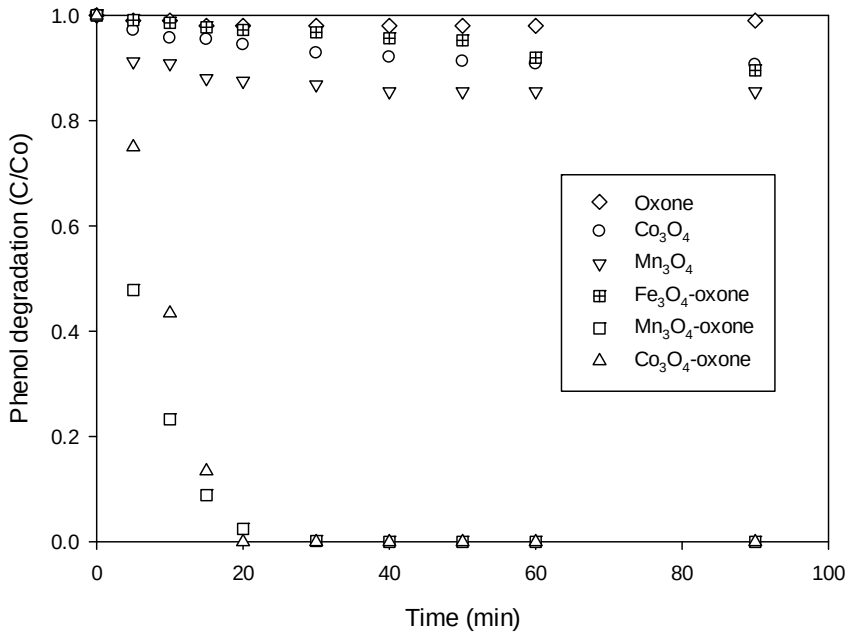

Figure 3. Phenol reduction with time in adsorption and catalytic oxidation. Reaction condition: [Phenol] = 25 mg/L, catalyst = 0.4 g/L, oxone = 2 g/L, and T = 25 ^{o}C.

3.3. Effects of reaction parameters on phenol degradation

The first parameter investigated in this study was phenol concentration, which was maintained at 25, 50, 75 or 100 mg/L. The effect of initial phenol concentration on phenol degradation is shown in Fig. 4. Overall, removal efficiency of phenol decreased with increasing phenol concentration. For Mn_3O_4, 100% degradation efficiency of phenol was achieved within 20 min at phenol concentration 25 mg/L, while in the same duration at phenol concentration of 50, 75 and 100 mg/L, degradation efficiency would only achieved at 96, 93 and 89%, respectively. A similar but more extended

variation could also be seen in Fig. 4b using Co_3O_4. At 25 mg/L phenol concentration, complete degradation of phenol was achieved within 20 min, while in the same duration at phenol concentration of 50, 75 and 100 mg/L, removal efficiencies obtained are 82, 58 and 51%, respectively. For phenol degradation in Mn_3O_4-oxone® and Co_3O_4-oxone®, phenol degradation is dependent on sulfate radicals. Due to the same concentrations of catalyst and oxidant, sulfate radical concentration produced in solution will be the same. Thus, high concentration of phenol in mixture will require more time to obtain the same removal rate, thus lowering phenol degradation efficiency.

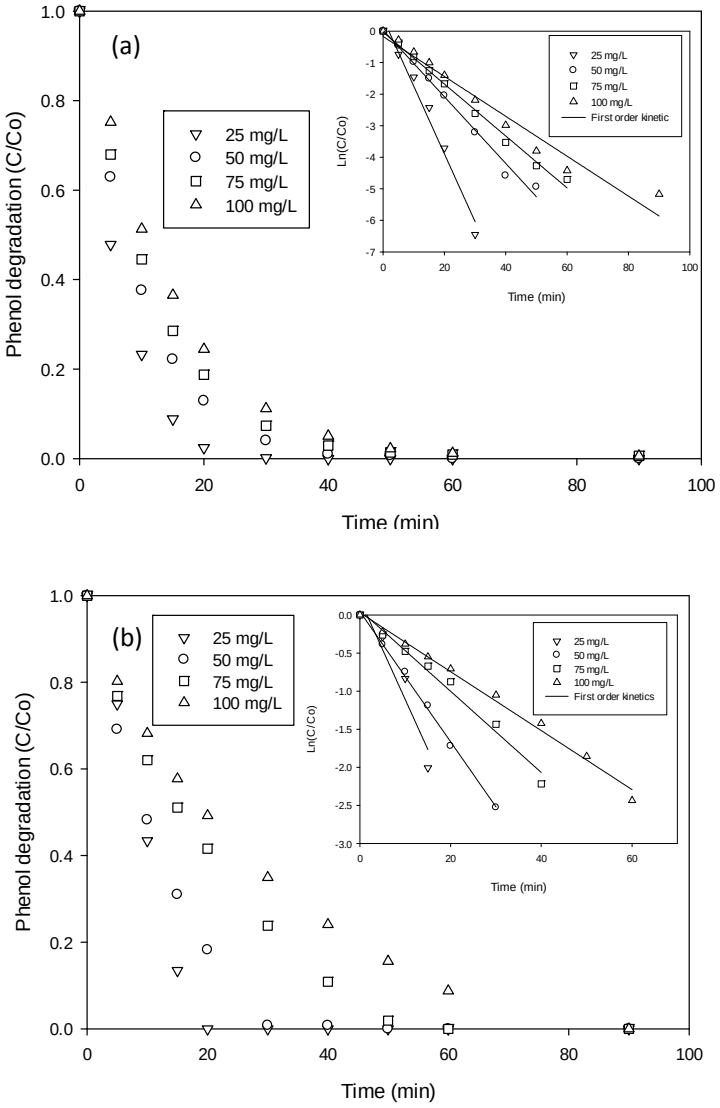

Figure 4. Effect of phenol concentration on phenol removal. (a) Mn_3O_4 and (b) Co_3O_4. Reaction condition: catalyst = 0.4 g/L, oxone = 2 g/L, and T = 25 ^oC.

In order to estimate the kinetic rates, a general pseudo first order kinetics for phenol degradation was employed, as shown in equation below.

$$\ln(C/C_0) = -k \bullet t \quad (3)$$

Where k is the apparent first order rate constant of phenol removal, C is the concentration of phenol at various time (t). C_o is the initial phenol concentration. Using this model to draw plots of ln(C/Co) versus time produced a straight line for four different phenol concentrations as shown in Fig. 4 (inset). Based on regression coefficients, it can be concluded that phenol degradation followed the first order kinetics. The rate constants at varying phenol concentrations for the two systems are shown in Table 2. As seen, rate constants will decrease as the concentration of phenol increases and Mn_3O_4 presented higher rate constants.

Table 2. Rate constant at different feed concentration of phenol

Catalyst	Initial phenol concentration (mg/L)	Rate constant (min^{-1})	R^2
Mn_3O_4	25	0.171	0.98
	50	0.102	0.99
	75	0.073	0.99
	100	0.068	0.96
Co_3O_4	25	0.092	0.91
	50	0.080	0.99
	75	0.053	0.98
	100	0.038	0.99

Fig. 5 presents phenol degradation efficiency at varying initial concentrations of oxone® in the solution. As can be seen, for both Mn_3O_4 and Co_3O_4 catalysts, the degradation of phenol depended on concentration of oxone®. Higher concentration of oxone® resulted in more removal of phenol. For Mn_3O_4, at 1.6 g/L oxone® loading, complete removal would be achieved in 50 min, while at

2.0 g/L oxone® loading, 100% removal efficiency would be achieved in 30 min. However, a further increase of oxone® loading in solution up to 2.4 g/L would not enhance the rate of reaction. In contrary, For Co_3O_4, the phenol degradation rate was increased when oxone® loading was decreased from 2.4 to 1.6 g/L. At 2.4 g/L oxone® loading, 84% removal efficiency would be achieved in 15 min, while in the same duration at 1.6 g/L oxone® loading, removal efficiency obtained is 99 %. For both Mn_3O_4 and Co_3O_4, an optimal oxone® loadings were achieved at 2.0 and 1.6 g/L, respectively. Based on stoichiometric reaction between phenol and oxone® (Eq. 4), the amount of oxone® needed for total mineralization of phenol is 2.2 g/L at 25 mg/L phenol. However, due to incomplete oxidation of phenol, optimal oxone® in this study seems to be lower than that in complete phenol mineralization.

$$C_6H_6O + 28\ HSO_5^- \longrightarrow 6\ CO_2 + 17\ H_2O + 28\ SO_4^{-\bullet} \quad (4)$$

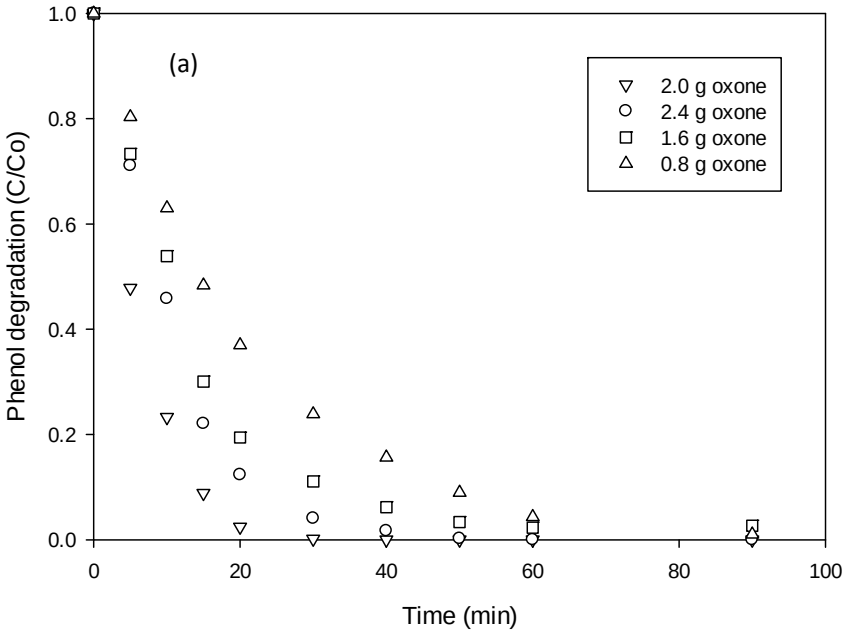

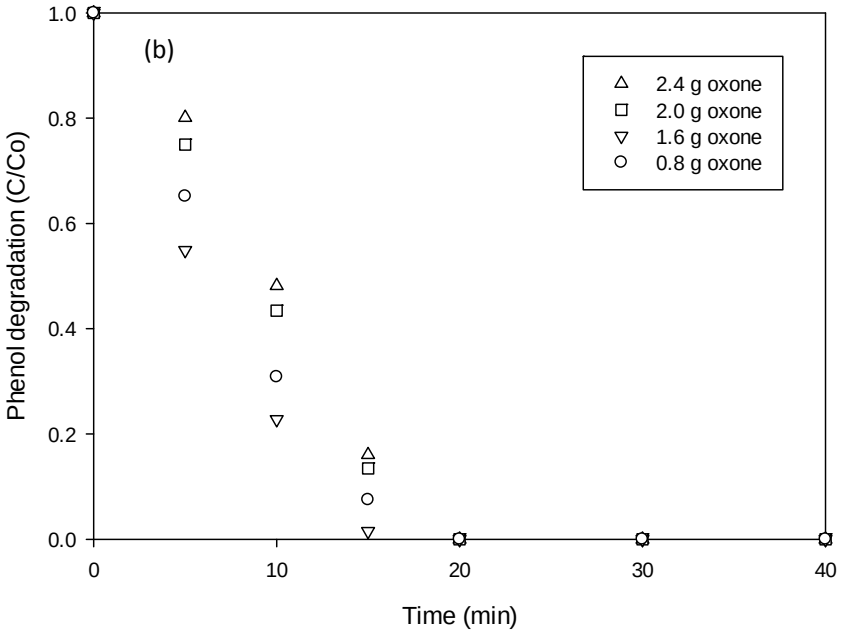

Figure 5. Effect of oxone concentration on phenol removal. (a) Mn_3O_4 and (b) Co_3O_4. Reaction condition: [phenol] = 25 mg/L, catalyst = 0.4 g/L, and T = 25 ^oC.

The effect of Mn_3O_4 and Co_3O_4 loading in solution on phenol degradation is shown in Fig. 6. Similar to the effect of oxone® loading, an increased amount of catalysts in the solutions enhanced phenol degradation efficiency. For Mn_3O_4, a complete removal of phenol could be reached within 30 min at 0.4 g/L catalyst loading. While in the same duration, 74, 63, and 50% removal could be reached at Mn_3O_4 loading of 0.3, 0.2, and 0.1 g/L, respectively. For Co_3O_4, phenol degradation rate was increased when catalyst loading was increased from 0.1 to 0.3 g/L. For instance, at 0.1 g/L catalyst loading, 48% degradation efficiency of phenol was achieved within 20 min while in the same duration, 70 and 100% removal efficiency could be reached at Co_3O_4 loading of 0.2 and 0.3 g/L, respectively. However, a further increase in Co_3O_4 loading in solution up to 0.4 g/L would not enhance the rate of reaction.

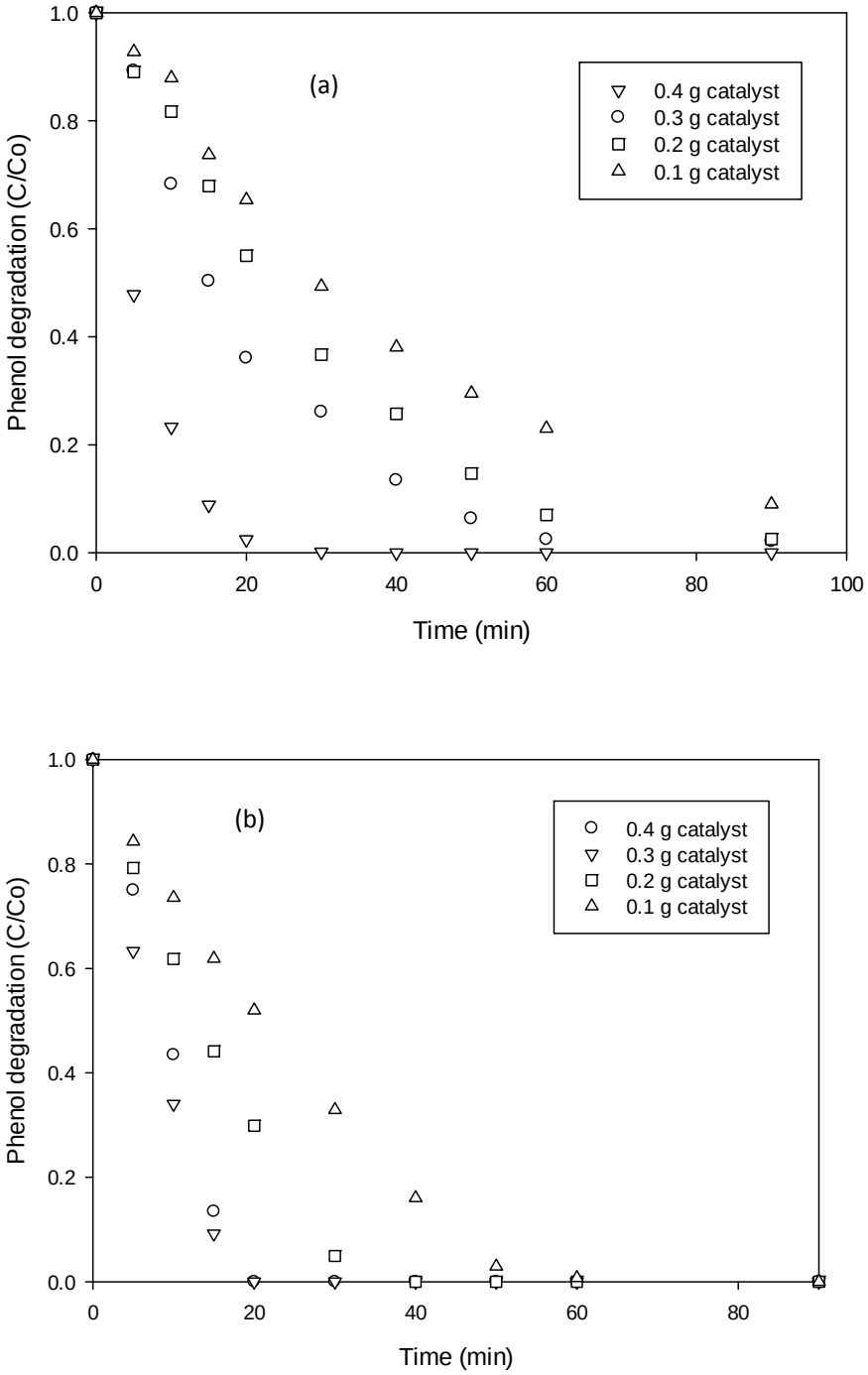

Figure 6. Effect of catalyst loading on phenol removal. (a) Mn_3O_4 and (b) Co_3O_4. Reaction condition: [phenol] = 25 mg/L, oxone = 2 g/L, and T = 25 ^{o}C.

In addition, reaction temperature is also a key factor influencing catalyst activity and phenol degradation. Fig. 7 shows the effect of temperature on phenol degradation. As can be seen, the rate of reaction would increase with temperature. For Mn_3O_4, complete phenol degradation at 25 ^oC would be achieved in 30 min. Further increase of 10 ^oC, 100% degradation efficiency of phenol was achieved within 20 min. At 45 ^oC, phenol removal would reach 100% at 10 min. A same profile was also obtained on Co_3O_4. Complete degradation efficiency of phenol at 15, 25, and 35 ^oC would be achieved in 40, 20 and 10 min, respectively. Using the first order kinetic rate constants and the Arrhenius equation, the activation energies of Mn_3O_4 and Co_3O_4 were derived as 38.5 and 66.2 kJ/mol, respectively. Compared with the activation energies of supported Co_3O_4 catalysts, Co/SiO_2 (61.7- 75.5 kJ/mol)[42], Co/AC (59.7 kJ/mol)[24], Co/Fly-ash (66.3 kJ/mol) [23] and Co/Red-mud (47.0 kJ/mol)[23], Co_3O_4 has the similar value while Mn_3O_4 has a much lower activation energy.

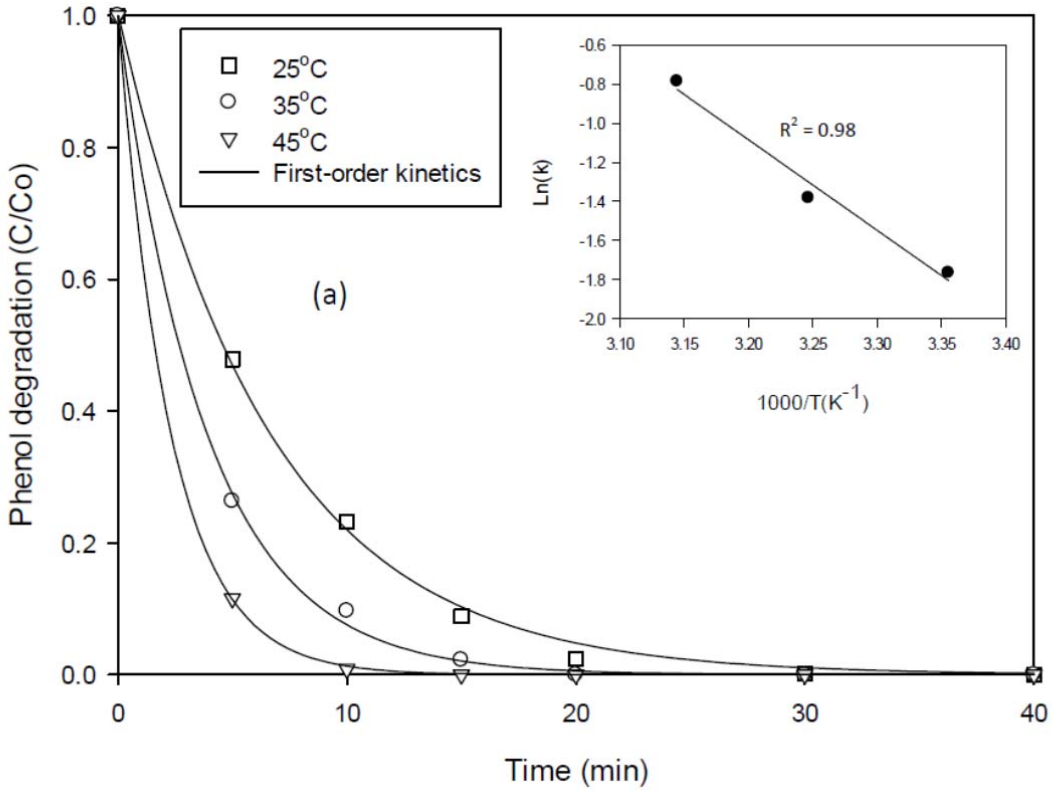

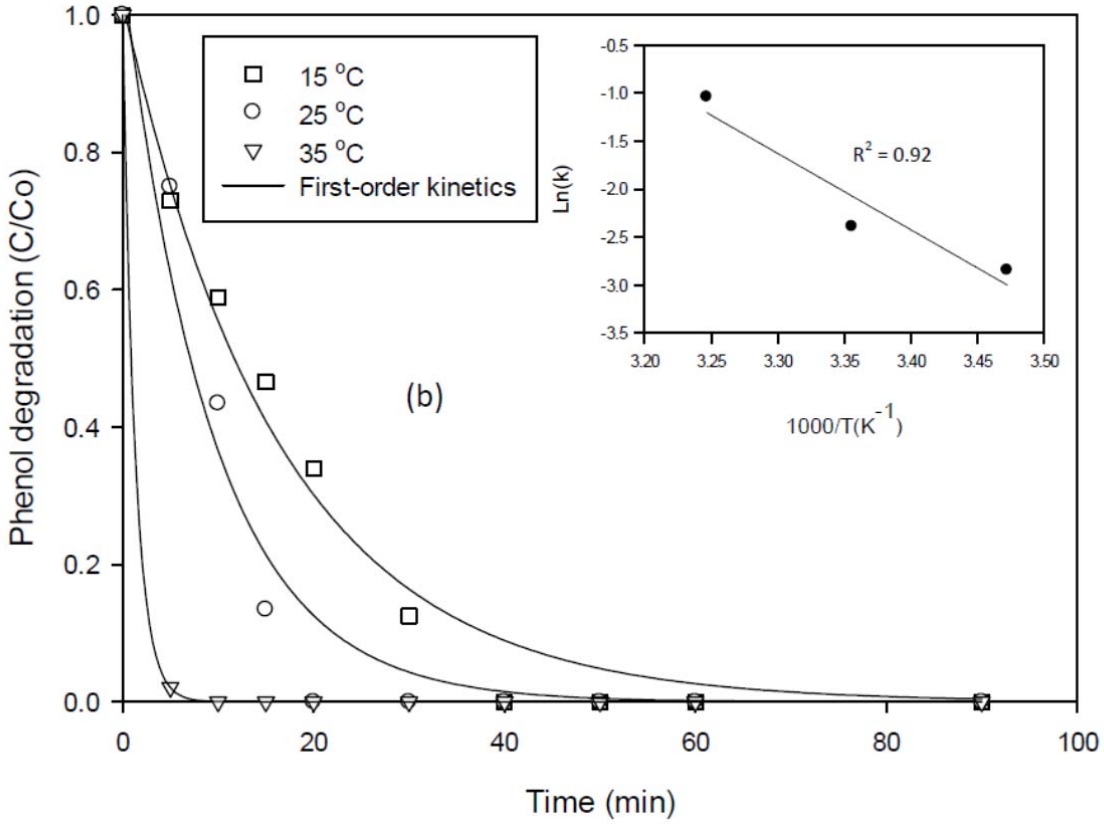

Figure 7. Effect of temperature on phenol removal. (a) Mn_3O_4 and (b) Co_3O_4. Reaction condition: [phenol] = 25 mg/L, catalyst = 0.4 g/L, and oxone = 2 g/L.

Fig. 8 further presents the performance of Mn_3O_4 and Co_3O_4 in phenol degradation after catalyst recycling with filtration and water washing. As can be seen, both catalysts, showed slight deactivation in the second and third runs. However, the deactivation was not significant. In the second and third runs, phenol degradation efficiencies at 40 min were much high at 100% and 98%, respectively for Mn_3O_4. For Co_3O_4, phenol degradation efficiencies at 40 min in the second and third runs were still at 100%. This suggests that Mn_3O_4 and Co_3O_4 are much stable and can be recycled for multiple uses.

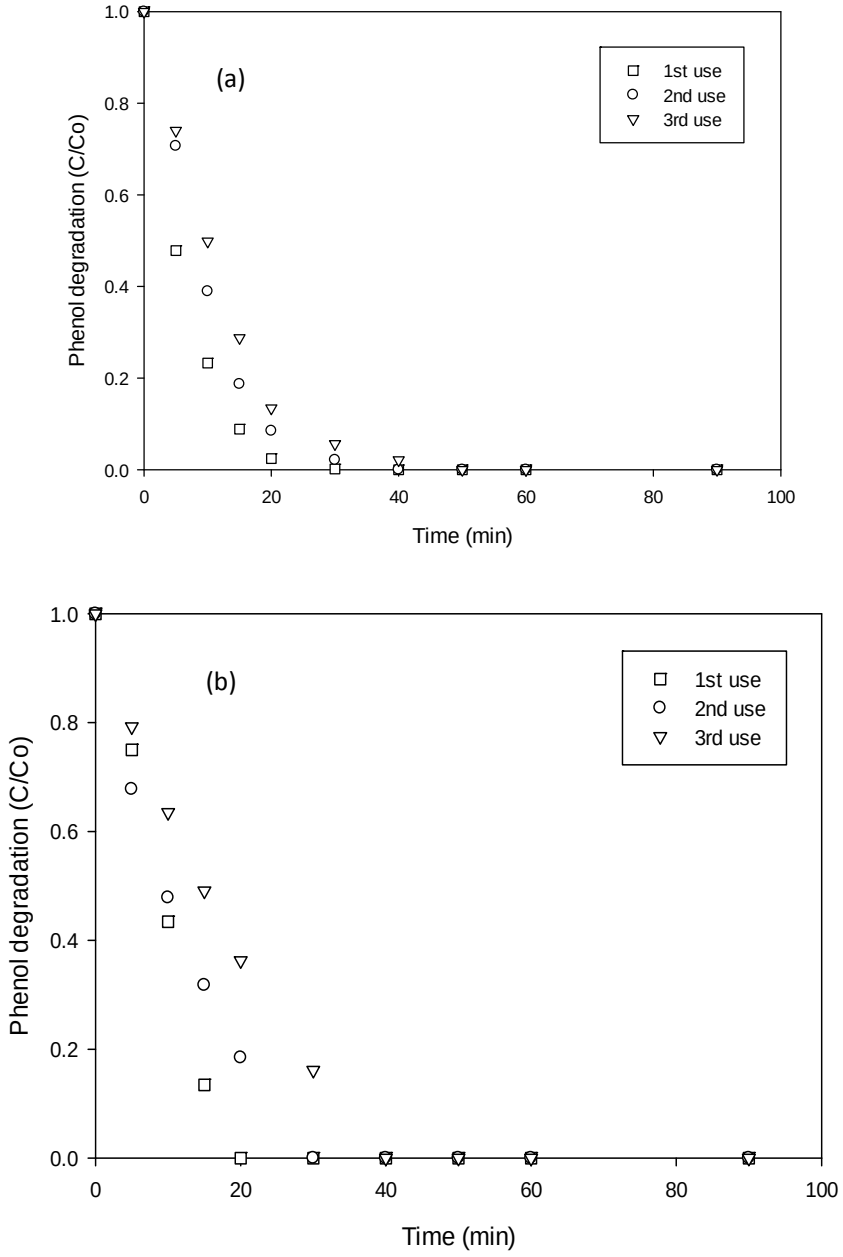

Figure 8. Degradation of phenol in multiple use of catalyst. (a) Mn_3O_4 and (b) Co_3O_4. Reaction condition: [phenol] = 25 mg/L, catalyst = 0.4 g/L, and oxone = 2 g/L.

4. Conclusions

Different spinel structured metal oxides, Mn_3O_4, Co_3O_4 and Fe_3O_4, were synthesized and compared in catalytic oxidation of phenol contaminant in water. Among them, Mn_3O_4 and Co_3O_4 are effective catalysts for generating sulfate radicals in the presence of oxone® to degrade phenol. The catalytic

activity follows the trend of Mn_3O_4 > Co_3O_4 > Fe_3O_4. For the reaction, higher catalyst and oxone® loadings would increase phenol degradation. Kinetic studies showed that phenol degradation followed first order reaction and activation energies on Mn_3O_4 and Co_3O_4 were obtained to be 38.5 and 66.2 kJ/mol, respectively. Mn_3O_4 also presented strong stability in catalytic performance in three runs, suggesting it can be used as a promising catalyst.

References

[1] V. Dohnal, D. Fenclova, J. Chem. Eng. Data, 40 (1995) 478-483.

[2] S.G. Christoskova, M. Stoyanova, M. Georgieva, Appl. Catal. A. 208 (2001) 243-249.

[3] A. Fortuny, C. Bengoa, J. Font, A. J. Hazard. Mater. 64 (1999) 181-193.

[4] M. Matheswaran, I.S. Moon, J. Ind. Eng. Chem. 15 (2009) 287-292.

[5] M. Bosnic, J.B. and, R.P. Daniels, United Nations Industrial Development Organization, (2000) 1-26.

[6] A. Marco, S. Esplugas, G. Saum, Water Sci. Technol. 35 (1997) 321-327.

[7] R. Andreozzi, V. Caprio, A. Insola, R. Marotta, Catal. Today, 53 (1999) 51-59.

[8] P. Bautista, A.F. Mohedano, J.A. Casas, J.A. Zazo, J.J. Rodriguez, J. Chem. Technol. Biotechnol. 83 (2008) 1323-1338.

[9] S. Wang, Dyes Pigments, 76 (2008) 714-720.

[10] H. Miyamura, R. Matsubara, Y. Miyazaki, S. Kobayashi, Ang. Chem. 119 (2007) 4229-4232.

[11] D.J. Cole-Hamilton, Science, 299 (2003) 1702-1706.

[12] G.P. Anipsitakis, D.D. Dionysiou, Environ. Sci. Technol. 37 (2003) 4790-4797.

[13] K.H. Chan, W. Chu, Water Res. 43 (2009) 2513-2521.

[14] X. Chen, X. Qiao, D. Wang, J. Lin, J. Chen, Chemosphere, 67 (2007) 802-808.

[15] J. Fernandez, P. Maruthamuthu, A. Renken, J. Kiwi, Appl. Catal. B. 49 (2004) 207-215.

[16] S.K. Ling, S. Wang, Y. Peng, J. Hazard. Mater. 178 (2010) 385-389.

[17] J. Madhavan, P. Maruthamuthu, S. Murugesan, M. Ashokkumar, Appl. Catal. A. 368 (2009) 35-39.

[18] A. Başoğlu, S. Parlayan, M. Ocak, H. Alp, H. Kantekin, M. Özdemir, Ü. Ocak, J. Fluoresc, 19 (2009) 655-662.

[19] G.P. Anipsitakis, E. Stathatos, D.D. Dionysiou, J. Phys. Chem. B. 109 (2005) 13052-13055.

[20] X. Chen, J. Chen, X. Qiao, D. Wang, X. Cai, Appl. Catal. B. 80 (2008) 116-121.

[21] P. Shukla, S. Wang, K. Singh, H.M. Ang, M.O. Tadé, Appl. Catal. B. 99 (2010) 163-169.

[22] S. Muhammad, E. Saputra, H. Sun, H.-M. Ang, M.O. Tadé, S. Wang, Ind. Eng. Chem. Res. 51 (2012) 15351-15359.

[23] E. Saputra, S. Muhammad, H. Sun, H.M. Ang, M.O. Tadé, S. Wang, Catal. Today, 190 (2012) 68-72.

[24] P.R. Shukla, S. Wang, H. Sun, H.M. Ang, M. Tadé, Appl. Catal. B. 100 (2010) 529-534.

[25] H. Liang, H. Sun, A. Patel, P. Shukla, Z.H. Zhu, S. Wang, Appl. Catal. B. 127 (2012) 330-335.

[26] W. Zhang, H.L. Tay, S.S. Lim, Y. Wang, Z. Zhong, R. Xu, Appl. Catal. B. 95 (2010) 93-99.

[27] Q. Yang, H. Choi, Y. Chen, D.D. Dionysiou, Appl. Catal. B. 77 (2008) 300-307.

[28] L. Hu, X. Yang, S. Dang, Appl. Catal. B. 102 (2011) 19-26.

[29] G. Zhou, H. Sun, S. Wang, H.M. Ang, M.O. Tade, Sep. Purif. Technol. 80 (2011) 626-634.

[30] Y. Yao, Z. Yang, D. Zhang, W. Peng, H. Sun, S. Wang, Ind. Eng. Chem. Res. 51 (2012) 6044-6051.

[31] Y. Yao, Z. Yang, H. Sun, S. Wang, Ind. Eng. Chem. Res. 51 (2012) 14958-14965.

[32] Q. Yang, H. Choi, S.R. Al-Abed, D.D. Dionysiou, Appl. Catal. B. 88 (2009) 462-469.

[33] S. Muhammad, P.R. Shukla, M.O. Tade, S. Wang, J. Hazard. Mater. 215 (2012) 183-190.

[34] E. Saputra, S. Muhammad, H. Sun, A. Patel, P. Shukla, Z.H. Zhu, S. Wang, Catal. Commun 26 (2012) 144-148.

[35] W. Zhang, Z. Yang, Y. Liu, S. Tang, X. Han, M. Chen, J. Crystal Growth, 263 (2004) 394-399.

[36] J. Jiang, J.P. Liu, X.T. Huang, Y.Y. Li, R.M. Ding, X.X. Ji, Y.Y. Hu, Q.B. Chi, Z.H. Zhu, Crystal Growth Design, 10 (2009) 70-75.

[37] Y. Zhai, J. Zhai, M. Zhou, S. Dong, J. Mater. Chem. 19 (2009) 7030-7035.

[38] G.P. Anipsitakis, D.D. Dionysiou, Environ. Sci. Technol. 38 (2004) 3705-3712.

[39] H. Liang, Y.Y. Ting, H. Sun, H.M. Ang, M.O. Tadé, S. Wang, J. Colloid Interface Sci. 372 (2012) 58-62.

[40] Y. Ding, L. Zhu, A. Huang, X. Zhao, X. Zhang, H. Tang, Catal. Sci. Technol. 2 (2012) 1977-1984.

[41] C. Chen, G. Ding, D. Zhang, Z. Jiao, M. Wu, C.-H. Shek, C.M.L. Wu, J.K.L. Lai, Z. Chen, Nanoscale, 4 (2012) 2590-2596.

[42] P. Shukla, H. Sun, S. Wang, H.M. Ang, M.O. Tadé, Sep. Purif. Technol. 77 (2011) 230-236.

List of Figures

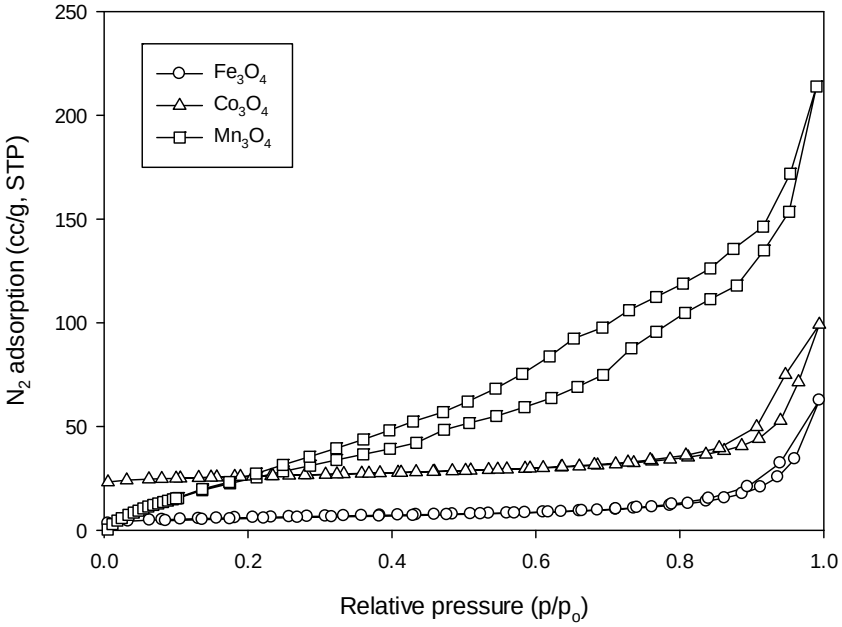

Fig. 1 N_2 adsorption isotherms of Fe_3O_4, Mn_3O_4, and Co_3O_4.

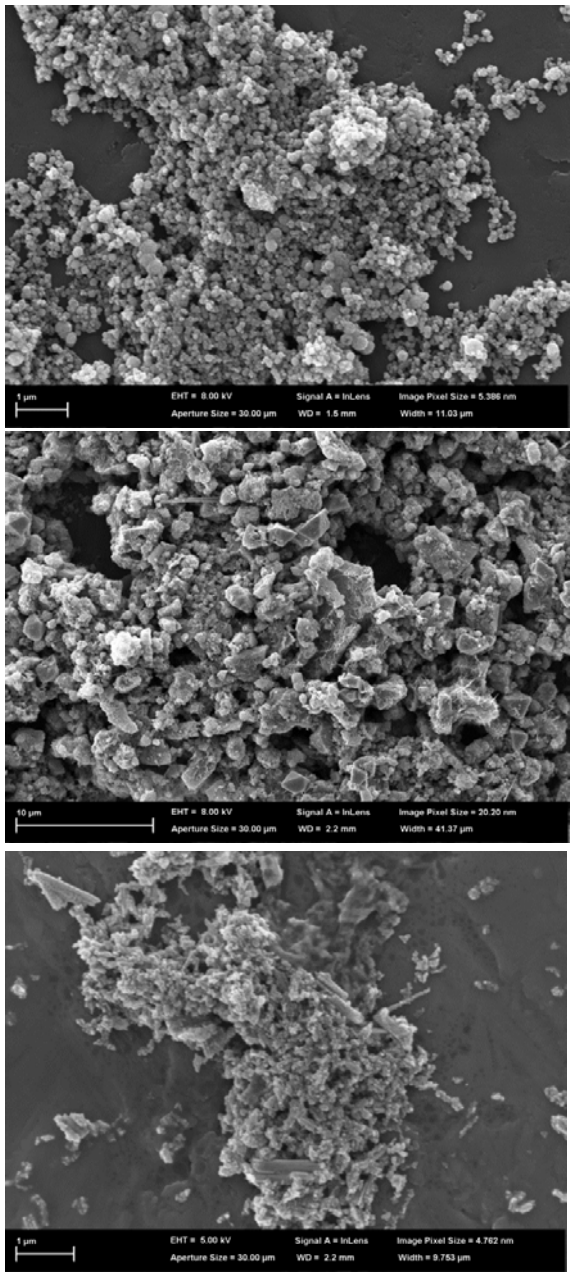

(a)

(b)

(c)

Fig. 2 SEM images of oxide catalysts. (a) Fe_3O_4, (b) Mn_3O_4, and (c) Co_3O_4.

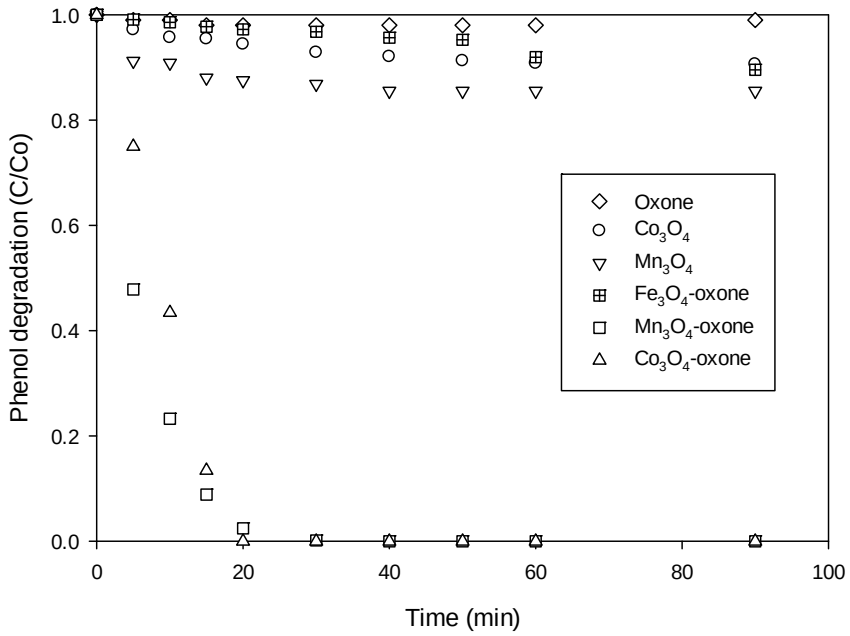

Figure 3. Phenol reduction with time in adsorption and catalytic oxidation. Reaction condition: [Phenol] = 25 mg/L, catalyst = 0.4 g/L, oxone = 2 g/L, and T = 25 ^{o}C.

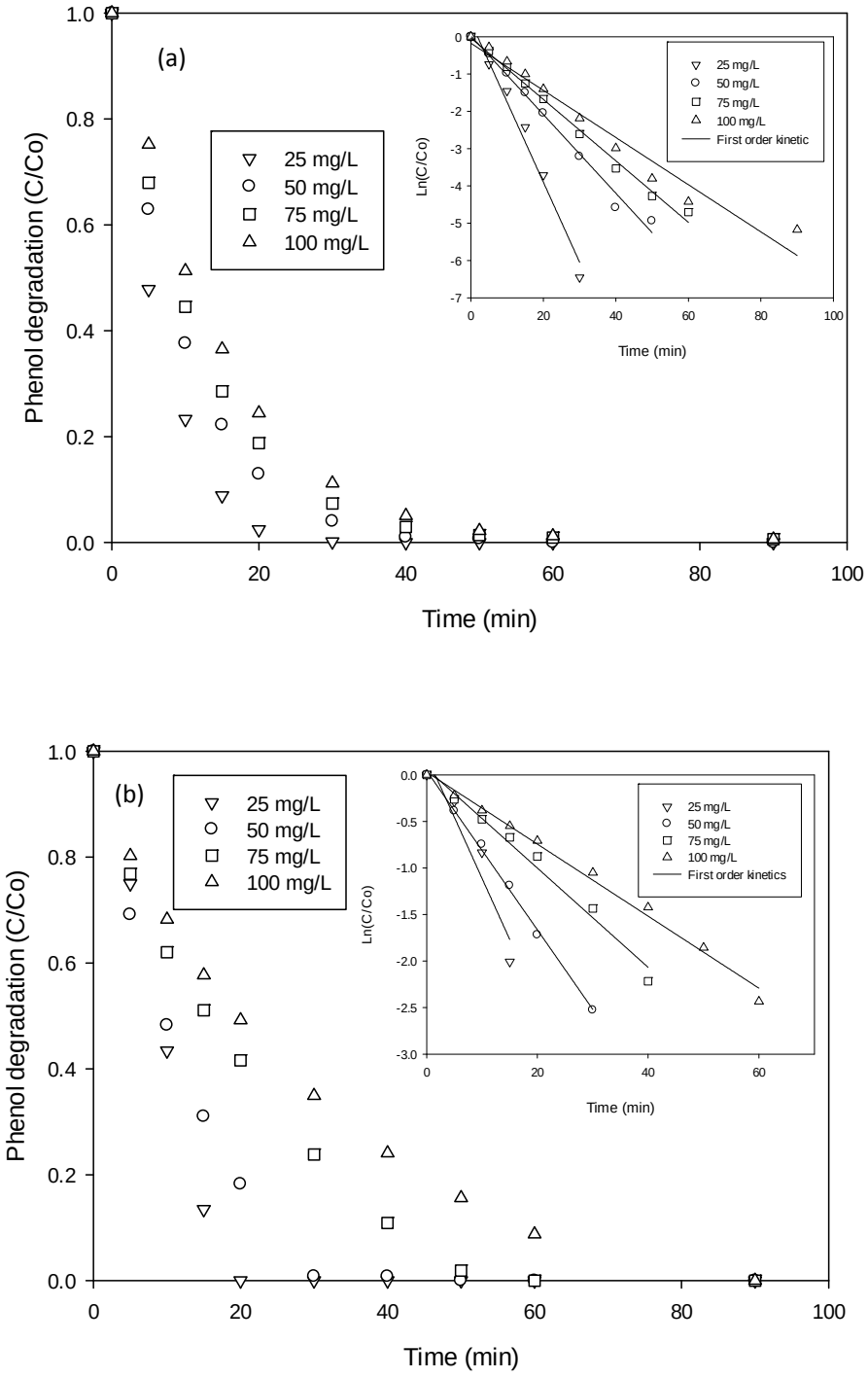

Figure 4. Effect of phenol concentration on phenol removal. (a) Mn_3O_4 and (b) Co_3O_4. Reaction condition: catalyst = 0.4 g/L, oxone = 2 g/L, and T = 25 ^{o}C.

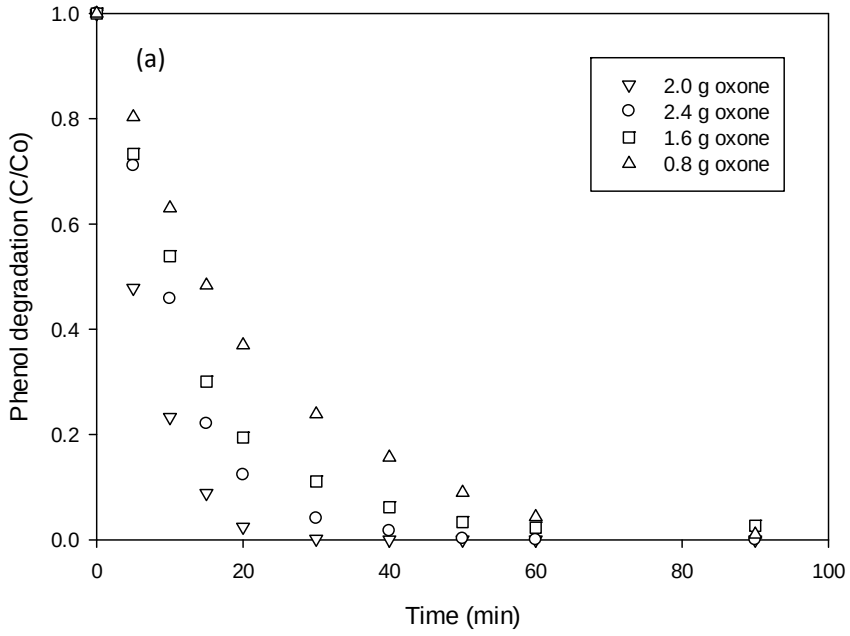

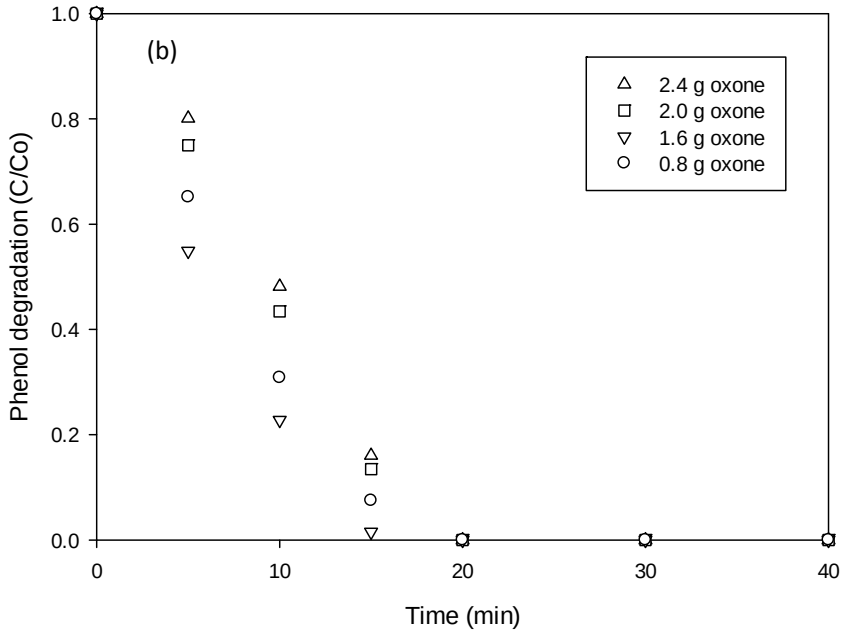

Figure 5. Effect of oxone concentration on phenol removal. (a) Mn_3O_4 and (b) Co_3O_4. Reaction condition: [phenol] = 25 mg/L, catalyst = 0.4 g/L, and T = 25 ^{o}C.

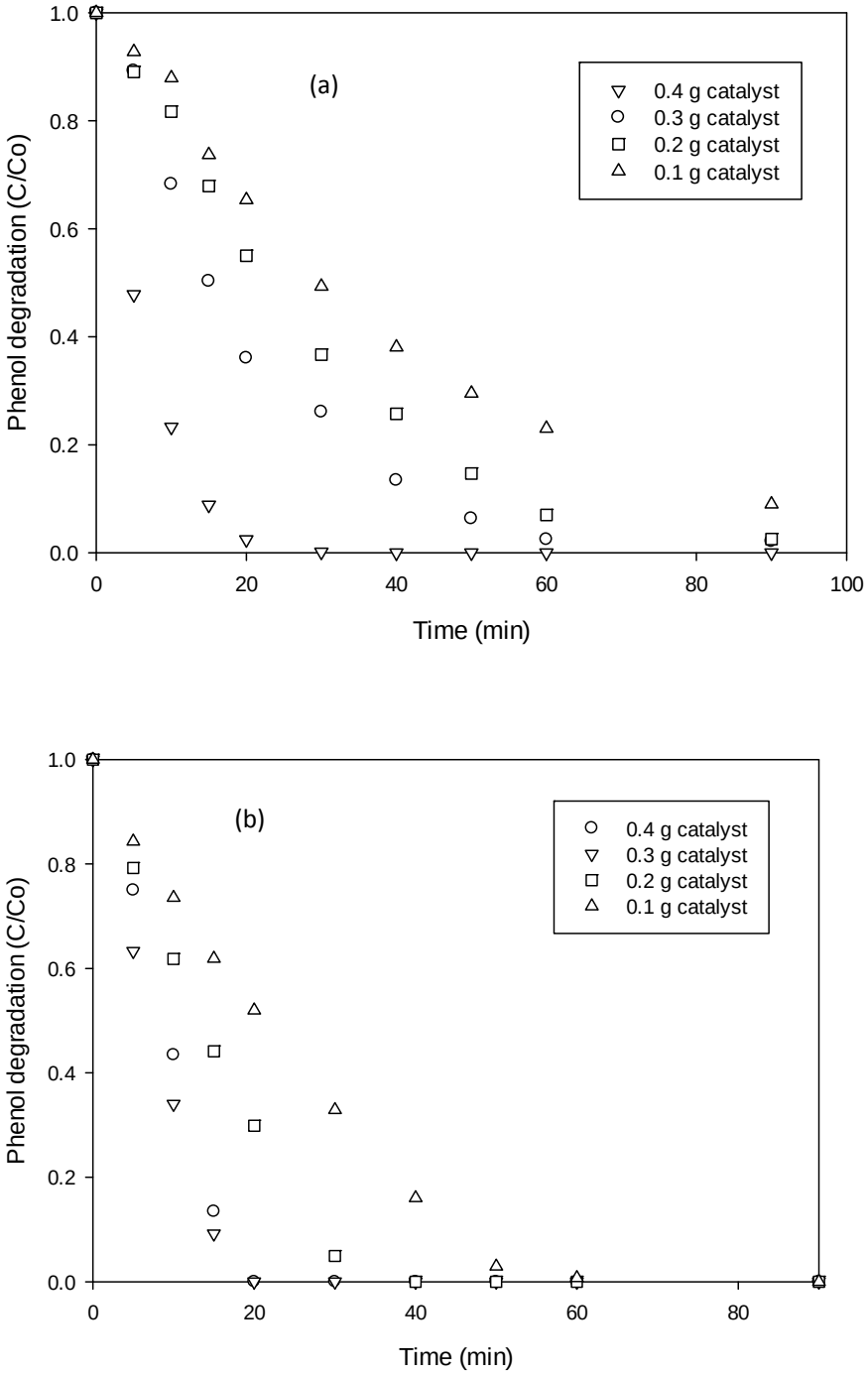

Figure 6. Effect of catalyst loading on phenol removal. (a) Mn_3O_4 and (b) Co_3O_4. Reaction condition: [phenol] = 25 mg/L, oxone = 2 g/L, and T = 25 ^{o}C.

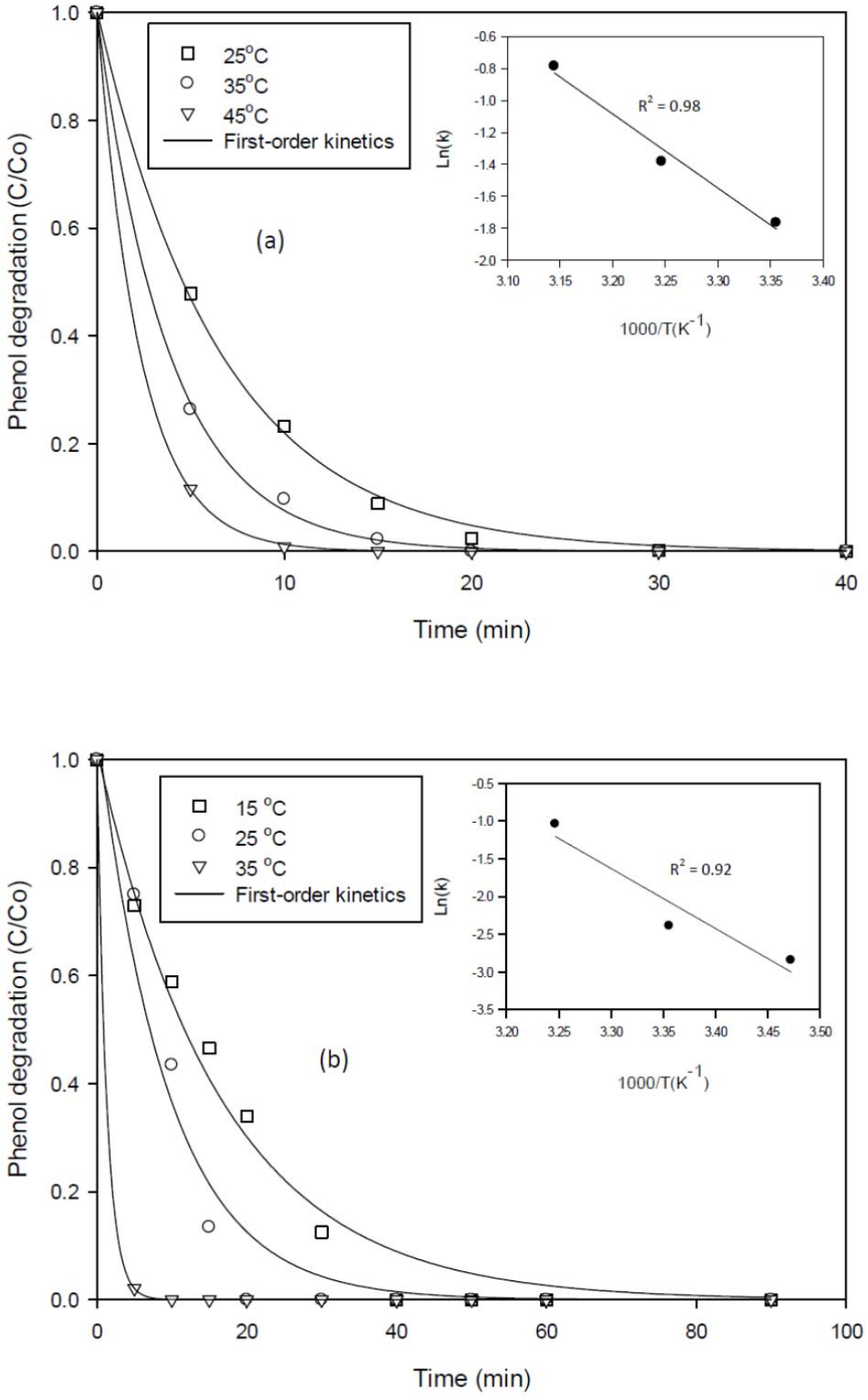

Figure 7. Effect of temperature on phenol removal. (a) Mn_3O_4 and (b) Co_3O_4. Reaction condition: [phenol] = 25 mg/L, catalyst = 0.4 g/L, and oxone = 2 g/L.

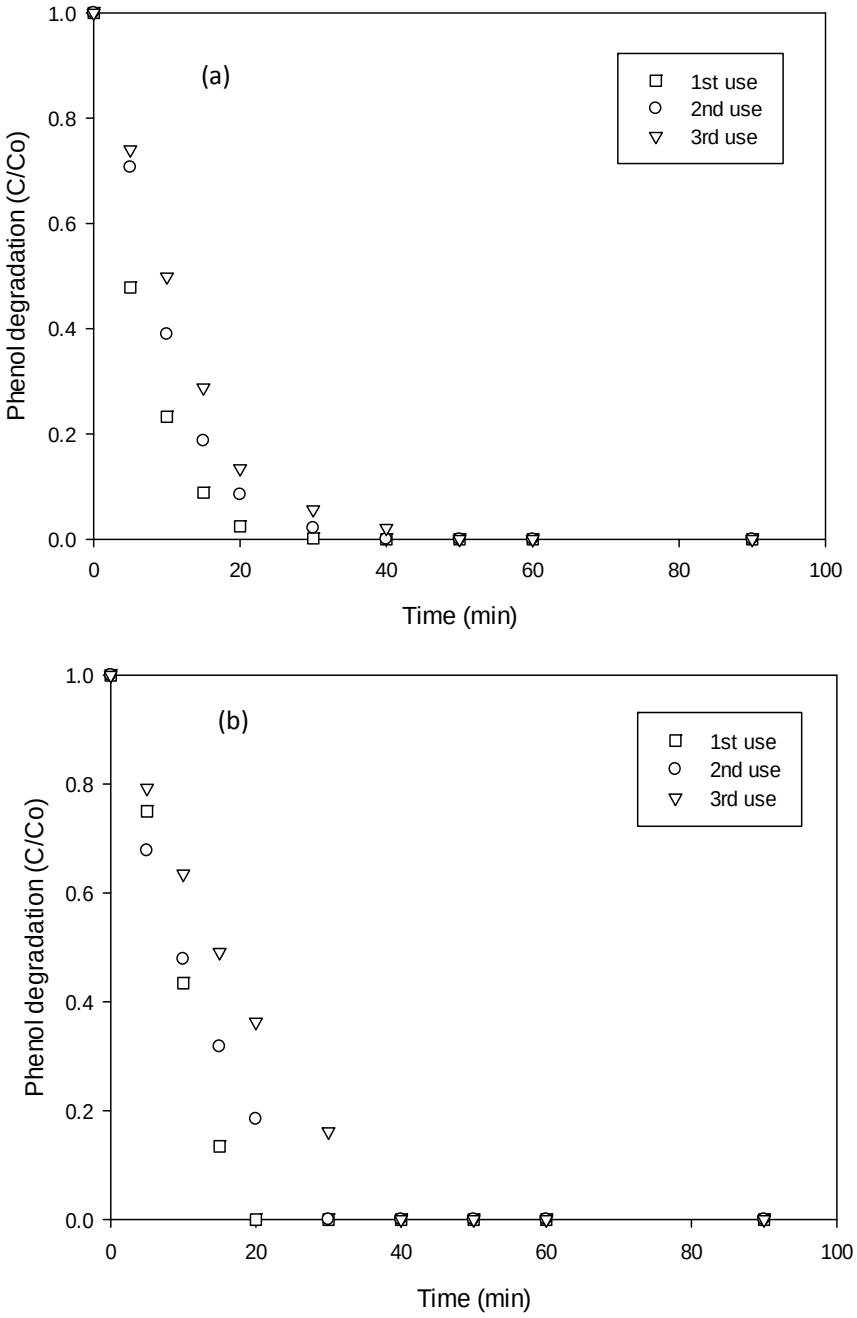

Figure 8. Degradation of phenol in multiple use of catalyst. (a) Mn_3O_4 and (b) Co_3O_4. Reaction condition: [phenol] = 25 mg/L, catalyst = 0.4 g/L, and oxone = 2 g/L.